Appl Magn Reson (2017) 48:1205–1217
DOI 10.1007/s00723-017-0931-8

Applied Magnetic Resonance

ORIGINAL PAPER

Modes and Fields of Two Stacked Dielectric Resonators in a Cavity of an Electron Paramagnetic Resonance Probe

Saba M. Mattar[1] · **Sameh Y. Elnaggar**[2]

Received: 13 July 2017 / Revised: 7 August 2017 / Published online: 30 August 2017

Abstract An electron paramagnetic resonance (EPR) probe consisting of two dielectric resonators (DRs) and a cavity (CV) is ideal for EPR experiments where both signal enhancement and tuning capabilities are required. The coupling of two DRs, resonating in their $TE_{01\delta}$ mode and a CV resonating in its TE_{011} mode, is studied using energy-coupled mode theory (ECMT). The frequencies and eigenvectors of the three coupled modes are analytically derived. As predicted numerically, ECMT confirms that the TE^{++-} and TE^{+--} modes are indeed found to be degenerate at a specific distance between the two DRs d_{12}. Additionally, the condition at which degeneracy occurs is specified. For a considerable range, the calculated frequency of the TE^{+++} mode changes linearly with respect to d_{12}. The TE^{+++} mode showed a 500 MHz frequency change over a distance of 2 cm, when the resonance frequency is around 9.7 GHz. This enables the experimentalist to linearly tune the probe over this large frequency range. Finally the asymmetric configuration, where one of the resonators (DR2) is kept at the cavity center and the other one is allowed to move along the cavity axis, is studied. It is estimated that the frequency changes by 600 MHz over a distance of 1.5 cm. A formula for the magnitude of the magnetic field along the cavity axis, where the EPR samples are usually placed, is developed. This is crucial in determining the magnetic field in the vicinity of the sample and the probe's filling factor.

✉ Saba M. Mattar
mattar@unb.ca

[1] Department of Chemistry and Centre for Laser, Atomic and Molecule Sciences, University of New Brunswick, Fredericton, NB E3B 5A3, Canada

[2] School of Engineering and Information Technology, University of New South Wales, Canberra, ACT 2600, Australia

1 Introduction

Spin-labeled analogs of biologically significant molecules and free radicals are usually large, while their paramagnetic centers, in comparison to their overall size, are small. Thus, they are paramagnetically dilute. In addition, the sample size is generally small and its quantity is limited. Consequently, extensive research and effort have been spent in increasing the sensitivity of the magnetic resonance spectrometers used to investigate these molecules. One way is to design more sensitive probes. Accordingly, miniature loop-gap (LGR) or dielectric (DR) resonators were introduced as probe components [1–5]. These resonators have small sizes, high energy density and large magnetic fields (B_1) in the sample vicinity, leading to large filling factors η. LGRs and DRs are normally housed in a shield to confine the probe's microwave radiation.

To this end we have derived, from first principles, an energy-conserved coupled mode theory (ECMT) to describe the properties of these probes and microwave resonators in general [6, 7]. Therefore, the frequencies, shape of the coupled modes, electric, and magnetic fields of probes were determined analytically and compared with full-wave finite element simulations [8]. Additional crucial general expressions of the probe parameters such as the quality factors, filling factors, and coupling coefficients among the resonators have been obtained [9, 10]. It is now possible to optimize dielectric and cavity configurations of a probe to maximize its efficiency parameter, Λ. One can now use the theoretical algebraic expressions derived from ECMT to build better probes and describe their properties at a wide frequency range.

Two stacked resonators in an electron paramagnetic resonance (EPR) probe add the flexibility of tuning the frequency over a certain frequency range [11–16]. Based on the Cohn model [17], doubly stacked dielectric resonators in free space and inside a shield were analyzed and the frequencies of the modes were calculated [18, 19]. In addition to their role as frequency tuners, the interaction of the two DRs within a CV improves the signal-to-noise ratio (SNR) of the detected EPR signal [13]. Experiments show that two stacked DRs, with a relative permittivity of $\varepsilon_r \approx 30$, inserted in a standard TE_{102} rectangular cavity improves the SNR approximately 24 times compared to that of the empty cavity [13].

To better understand the interactions between two DRs in a CV, the coupling was previously studied using numerical simulations [12]. It was found that the interaction of the two $TE_{01\delta}$ DR modes and the CV TE_{102} mode results in three coupled ones. They were designated as the TE^{+++}, TE^{++-} and TE^{+--} modes. The "+"and "−" signs refer to in-phase and out-of-phase interactions between the original two $TE_{01\delta}$ and TE_{102} modes, respectively. The fields of all three modes were numerically computed and described in detail [12]. It was observed that the TE^{+--} mode is completely dielectric in nature, where the cavity has no effect on the coupling. Consequently it was concluded that it is hard to excite this mode via an iris on the surface of the cavity side-wall [12]. On the other hand, the magnetic field of the TE^{+++} mode has a CV component and hence can be excited by an iris. Additionally, the mode frequency changes linearly with respect to the distance (d_{12}) between the two DRs. This observation can be used to design frequency-tuneable

probes. Numerically calculated mode frequencies were found to be in excellent agreement with measurements [12]. The computations also showed that the TE^{++-} and TE^{+--} modes become degenerate at a specific distance between the DRs.

In this article, we exploit ECMT to rigorously determine the coupled modes of an EPR probe, which consists of two stacked DRs inserted in a conducting CV. The numerically and experimentally observed modes, frequency change, and field distributions, are discussed in detail. Although the analysis carried out here is quite general, a cylindrical CV resonating in its TE_{011} mode is used, since it enables us to obtain closed form expressions. Based on ECMT, the dependence of resonant frequencies on the separation distance between the DRs (d_{12}) is attributed to the coupling terms, which have clear physical interpretations [20]. Specifically, the reason behind the degeneracy of the two higher modes becomes apparent and is precisely defined. Additionally, we derive a useful linearized formula for the frequency change of the TE^{+++} mode versus d_{12}, used in EPR measurements [12, 13].

Finally, the asymmetric configuration of the two DRs in the CV is investigated. In this configuration, one of the DRs is kept at the CV center to hold the sample, while the other acting as a frequency tuner, is allowed to move along the cavity's $D_{\infty h}$ axis of highest symmetry. The frequency shifts of the TE^{+++} mode are then calculated using ECMT and verified using finite element simulations.

Section 2 presents the probe structure and applies ECMT to determine closed form expressions for the coupled eigenmode frequencies and fields. In Sect. 3, these expressions and full-wave finite element simulations are applied to typical structures and scenarios. The condition at which degeneracy occurs is also derived and, more importantly, the trend of the frequency of the TE^{+++} mode as a function of the separation distance d_{12}, is presented. Finally, Sect. 4 summarizes the main conclusions and implications.

2 Theoretical Analysis

The probe under consideration is depicted in Fig. 1. It consists of two cylindrical DRs with moderately high relative permittivity ($\varepsilon_r = 29.2$) placed in a cylindrical

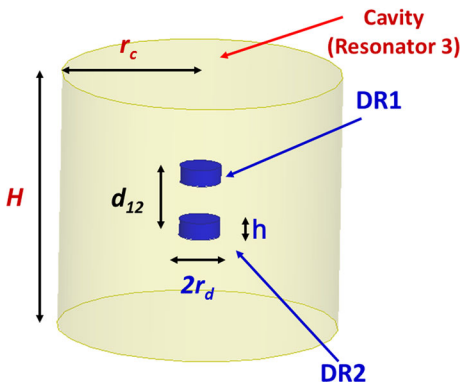

Fig. 1 Two dielectric resonators in a cylindrical cavity. The resonators are held in a tube with a low-loss and low-dielectric constant material not shown in the figure. $H = 4.1$ cm, $r_c = 2.05$ cm, $h = 2.65$ mm, and $r_d = 3$ mm

TE_{011} CV. The holder, not shown in the figure, is a tube made from a low-loss and low-relative permittivity, such as Teflon®, and hence its effect is small [12]. The cylindrical symmetry of this structure makes it possible to find closed form expressions for the coupling coefficients between the two DRs and the CV [9]. The system is similar to that previously discussed where a rectangular TE_{102} CV was used instead [12]. The height and radius of the CV are 4.1 cm. Similarly, the height and radius of the DRs are 2.65 and 3.0 mm, respectively. These dimensions guarantee that the three components have the same resonant frequency.

A simplified eigenvalue equation of the three coupled system can be determined after inspecting the rather simpler case of one DR (DR1) in a CV (resonator 3), which was found to be [8]:

$$\begin{pmatrix} \omega_0^2 & -\omega_0^2\kappa_{13} \\ -\omega_0^2\kappa_{31} & \omega_0^2 \end{pmatrix} \begin{pmatrix} a_1 \\ a_3 \end{pmatrix} = \omega^2 \begin{pmatrix} a_1 \\ a_3 \end{pmatrix},$$

where $\kappa_{13} = \kappa_{31}$ is the coupling coefficient between DR1 and CV. After the introduction of DR2, the augmented eigenvalue equation becomes:

$$\begin{pmatrix} \omega_0^2 & -\omega_0^2\kappa_{12} & -\omega_0^2\kappa_{13} \\ -\omega_0^2\kappa_{21} & \omega_0^2 & -\omega_0^2\kappa_{23} \\ -\omega_0^2\kappa_{31} & -\omega_0^2\kappa_{32} & \omega_0^2 \end{pmatrix} \begin{pmatrix} a_1 \\ a_2 \\ a_3 \end{pmatrix} = \omega^2 \begin{pmatrix} a_1 \\ a_2 \\ a_3 \end{pmatrix}. \tag{1}$$

Here $\kappa_{12}(\kappa_{21})$ is the coupling coefficient between the two dielectric resonators and $\kappa_{i3}(\kappa_{3i})$ is the coupling coefficient between the ith dielectric and the cavity, where $\kappa_{ij} = \kappa_{ji}$ [20].

2.1 Modes of Symmetrically Placed DRs

When the two dielectrics are symmetrically placed, $\kappa_{13} = \kappa_{23}$. It is convenient to define $\alpha \equiv \frac{\kappa_{12}}{\kappa_{13}}$ and $\kappa \equiv \kappa_{13}$, therefore, one can rewrite Eq. (1) as:

$$\omega_0^2 \begin{pmatrix} 1 & -\alpha\kappa & -\kappa \\ -\alpha\kappa & 1 & -\kappa \\ -\kappa & -\kappa & 1 \end{pmatrix} \begin{pmatrix} a_1 \\ a_2 \\ a_3 \end{pmatrix} = \omega^2 \begin{pmatrix} a_1 \\ a_2 \\ a_3 \end{pmatrix}.$$

Solving the above eigenvalue problem, the eigenvalues and the corresponding eigenvectors for the coupled system are found to be:

$$\omega_{+++}^2 = \omega_0^2 \left(1 - \frac{1}{2}\alpha\kappa - \frac{1}{2}\sqrt{\alpha^2\kappa^2 + 8\kappa^2}\right), \tag{2}$$

$$\omega_{++-}^2 = \omega_0^2 \left(1 - \frac{1}{2}\alpha\kappa + \frac{1}{2}\sqrt{\alpha^2\kappa^2 + 8\kappa^2}\right), \tag{3}$$

$$\omega_{+--}^2 = \omega_0^2(1 + \alpha\kappa), \tag{4}$$

$$\mathbf{a}_{+++} = \left(\frac{3\alpha + \sqrt{\alpha^2 + 8}}{-\alpha^2 + \alpha\sqrt{\alpha^2 + 8} + 4}, \quad \frac{3\alpha + \sqrt{\alpha^2 + 8}}{-\alpha^2 + \alpha\sqrt{\alpha^2 + 8} + 4}, \quad 1 \right)^{\dagger}, \tag{5}$$

$$\mathbf{a}_{++-} = \left(\frac{-3\alpha + \sqrt{\alpha^2 + 8}}{\alpha^2 + \alpha\sqrt{\alpha^2 + 8} - 4}, \quad \frac{-3\alpha + \sqrt{\alpha^2 + 8}}{\alpha^2 + \alpha\sqrt{\alpha^2 + 8} - 4}, \quad 1 \right)^{\dagger}, \tag{6}$$

and

$$\mathbf{a}_{+--} = (1, \ -1, \ 0)^{\dagger}. \tag{7}$$

2.2 TE^{+++} Mode of Asymmetrically Placed DRs

A tuneable doubly stacked probe can be formed by placing the two DRs asymmetrically inside the CV. In this configuration, one of the DRs (DR2, for example) is fixed at the CV center and DR1 is placed anywhere along the CV axis and thus acts as a frequency tuner. As was shown by numerical calculations and direct measurements such configuration enhances the signal-to-noise ratio, while allowing the resonant frequency to be tuned over a considerable frequency range [12, 13]. According to the Cohn model, κ_{12} decreases exponentially as d_{12} is increased [17]. Hence when d_{12} is large enough, the direct interaction between the two DRs can be ignored ($\kappa_{12} = 0$). Accordingly, the eigenvalue and eigenvector of the TE^{+++} mode become:

$$\omega_{+++}^2 = \omega_0^2 \left(1 - \kappa\sqrt{1 + \beta^2} \right), \tag{8}$$

and

$$\mathbf{a}_{+++} = \left(\frac{\beta}{\sqrt{\beta^2 + 1}}, \quad \frac{1}{\sqrt{\beta^2 + 1}}, \quad 1 \right)^{\dagger}. \tag{9}$$

Here $\kappa = \kappa_{23}$ is the coupling coefficient between DR2 and CV, and $\beta\kappa = \kappa_{13}$ is the coupling coefficient between DR1 and CV.

3 Results and Discussion

In this section, the expressions derived in the previous section are used to explain the behavior of the coupled modes. In Sect. 3.1, we discuss the symmetric case; the asymmetric case is examined in Sect. 3.2

3.1 Symmetrically Placed DRs

The probe in Fig. 1 is simulated when the DRs are symmetrically placed in the CV using the HFSS® eigenmodes solver (Ansys Corporation, Pittsburgh, PA, USA). In this configuration $d_{12} = 2$ mm; the fields' distributions of the three coupled modes

are depicted in Fig. 2. The magnetic field, B_1, distributions in Fig. 2a and c look similar and are delocalized. However, B_1 in Fig. 2a is more homogeneous in the vicinity of the two DRs. This is because the three uncoupled modes forming the TE^{+++} mode in Fig. 2a are all in phase; unlike the TE^{++-} mode, where the CV mode is out of phase. On the other hand, Fig. 2b clearly shows that the TE^{+--} mode is completely dielectric in nature and the cavity does not contribute to the coupling. This agrees with the ECMT predictions given by Eqs. (4) and (7). Furthermore, (Eq. 7) predicts that this mode is purely anti-symmetric. Since the cavity field is in phase with the mode of one dielectric and out of phase with the other, the coupled energy injected by the CV to one of the dielectric modes is equal to that pumped out to the CV via the other dielectric mode, leaving zero net energy in the CV mode.

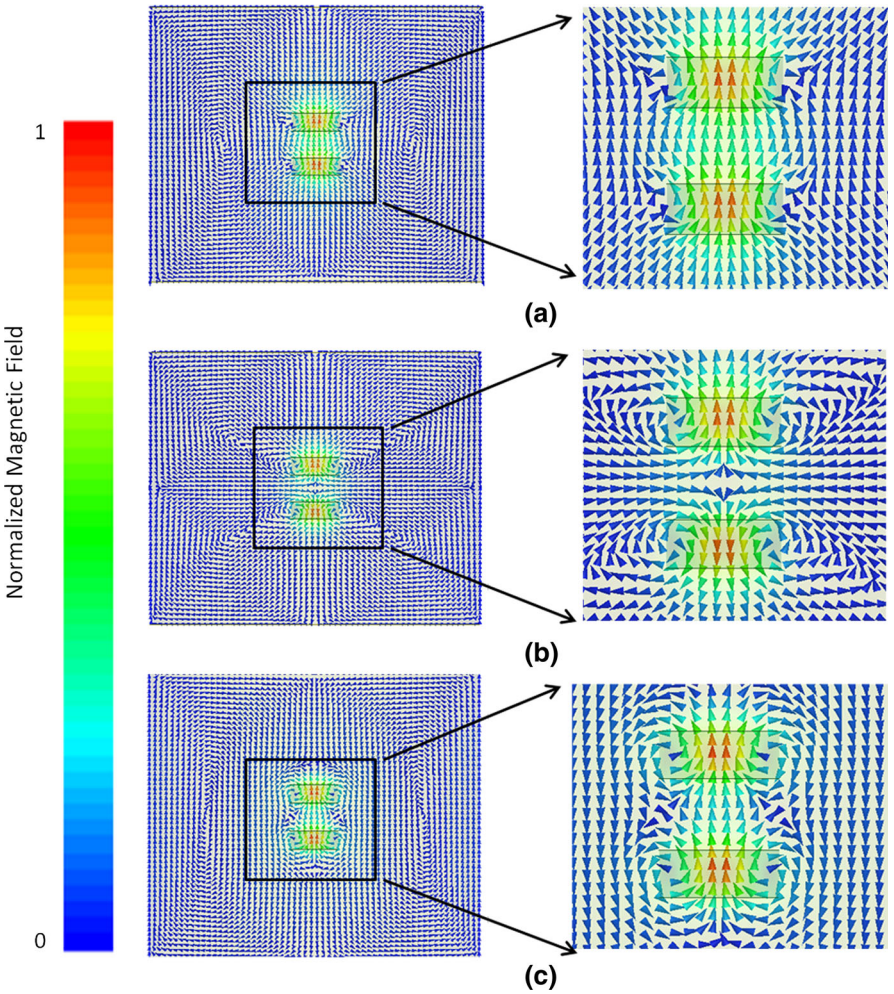

Fig. 2 Magnetic field distributions of the three coupled modes. **a–c** Illustrate the TE^{+++}, TE^{+--}, TE^{++-} modes, respectively

Such a situation is not uncommon; for example when a relay coil is inserted between two inductively resonant coils, the relay coil transfers energy from the one resonant coil to the other without itself storing energy. Such a phenomenon is called electromagnetically induced transparency (EIT) [21] and was exploited to show that electric power can be wirelessly transferred over a considerably large distance [22].

One of the most significant and desirable properties of probes consisting of two DRs is the capability to tune the resonant frequency by controlling d_{12}. To quantify how the frequency depends on d_{12}, we resort to Eqs. (2)–(4) to calculate the frequencies of the three coupled modes. The results are compared to HFSS simulations as presented in Fig. 3. One can see that the upper two modes (TE^{++-} and TE^{+--}), irrespective of the method of calculation, can be degenerate at some particular d_{12}. Equating (3) to (4), the condition at which the two modes are degenerate is found to be:

$$\alpha = 1 \text{ or } \kappa_{12} = \kappa_{13}. \tag{10}$$

The eigenvector for the TE^{++-} mode when $\alpha = 1$ is:

$$\frac{1}{\sqrt{6}}(-1 \quad -1 \quad 2)^{\dagger}.$$

In Fig. 3, the κ_{12} parameter was calculated using the Cohn model [17], which becomes less accurate outside the dielectric material, particularly for relatively moderate ε_r. This is because it is assumed that the side walls (curved surfaces) of the DR are perfect magnetic walls. Accordingly in Fig. 3, condition Eq. (10) is met at $d_{12} = 1.5$ mm, which is different from the finite element simulated value ($d_{12} = 2.2$ mm). However, a more accurate κ_{12} can be determined using the frequency splitting formula of the two DRs when placed d_{12} apart in free space [23]:

$$\kappa_{12} = \frac{\omega_{+-}^2 - \omega_{++}^2}{\omega_{+-}^2 + \omega_{++}^2}. \tag{11}$$

The symmetric and anti-symmetric frequencies, ω_{++} and ω_{+-}, are determined from the simulation of the eigenvalues of the two DRs only. Equation (11) is then used to estimate a more accurate value of κ_{12} as the solid curve in Fig. 4 shows. It is clear from this figure that κ_{12} decreases in an exponent-like fashion, consistent with

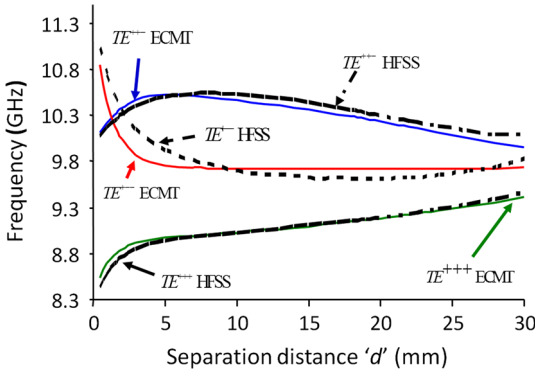

Fig. 3 Frequency of the coupled modes versus the separation distance d_{12}

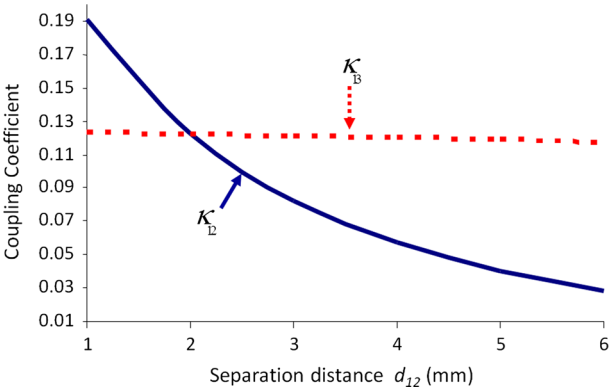

Fig. 4 Coupling coefficients κ_{12} and κ_{13} plotted for various separation distance d_{12}

the evanescent field assumption used in the Cohn model outside of the flat (upper and lower) DR surfaces. An analytical closed form expression for the cavity-DR1 coupling coefficient, κ_{13}, can be found based on one DR placed at the CV center [9]. Taking into account that the electric field of the CV TE_{011} mode is maximum at the CV mid-plane and decreases sinusoidally toward the upper (lower) flat boundaries, κ_{13} for an arbitrary distance d_{12} is found to be:

$$\kappa_{13} = 13.16 \frac{(\varepsilon_r - 1)}{\sqrt{2\varepsilon_r k_d H}} \frac{A_D}{A_C} \sqrt{\frac{1 - \cos k_d h}{\beta h + \sin k_d h}} \cos\left(\frac{\pi}{2H}(d_{12} + h)\right). \tag{12}$$

Here A_D and A_C are the dielectric and cavity base areas, respectively, and k_d is the dielectric wave number in the z-direction. Equation (12) is plotted in Fig. 4. For small values of d_{12} ($d_{12} \ll H$), κ_{13} is practically constant. When the two modes are degenerate ($\kappa_{12} = \kappa_{13}$), the plot shows that d_{12} is at 2 mm. This is a more accurate value than the one predicted relying on the Cohn model (1.5 mm).

Previously, the TE^{+++} mode was used in EPR experiments. It was shown that by exploiting this mode, the signal-to-noise ratio is enhanced by 24 times besides the capability of tuning the resonant frequency over a considerable range [12, 13]. Figure 3 shows that the frequency of the $TE^{+++} - d_{12}$ curve is approximately linear beyond the degeneracy point where $\kappa_{13} > \kappa_{12}$. In this range, when $\kappa_{13} \ll 1$, the frequency given by Eq. (2) can be written as the approximately linear form:

$$\omega_{+++} \approx \omega_0 \left(1 - \sqrt{2}\kappa_{13}\right)^{\frac{1}{2}} \approx \omega_0 \left(1 - \frac{\sqrt{2}}{2}\kappa_{13}\right). \tag{13}$$

Equation (13) indicates that the effective coupling coefficient, $\kappa'_{13} = \sqrt{2}\kappa_{13}$, is larger than that when only one DR is inserted in the same position of one of either the two dielectrics DR1 or DR2. From Eq. (12) and noting that $d_{12} \gg h$, the coupling coefficient κ_{13} can be written as:

$$\kappa_{13} = \kappa_{13}^{0} \cos\left(\frac{\pi d_{12}}{2H}\right), \tag{14}$$

where κ_{13}^{0} is the coupling coefficient when the DR is located at the cavity center. Using Eq. (14), the frequency ω_{+++} can be linearized around $d_{12} = H/2$ to give:

$$\omega_{+++} \approx \omega_0\left(1 - \frac{\kappa_{13}^{0}}{2} + \frac{\kappa_{13}^{0}\pi}{4H}x\right) \approx \omega_0\left(1 - \frac{\kappa_{13}^{0}}{2} - \frac{\kappa_{13}^{0}\pi}{4} + \frac{\kappa_{13}^{0}\pi d_{12}}{4H}\right), \tag{15}$$

where $x = (d_{12} - H)/2$. The approximate relation between ω^{+++} and d_{12} in Eq. (15) is plotted in Fig. 5. Indeed it clearly shows that the frequency is fairly linear over a frequency span of 500 MHz when d_{12} changes by 2 cm. Equation (15) also suggests that to increase the tuneable range, one can decrease the CV height and/or increase the coupling between the CV and the DR when inserted at the CV center.

3.2 Asymmetrically Placed DRs

In Ref. [12] it was demonstrated that if the dielectrics were asymmetrically placed in a TE_{102} rectangular cavity, one of the DR houses the sample, while the other one acts as a frequency tuner. Using Eq. (14), the parameter β appearing in Eq. (8) is found to be:

$$\beta = \cos\left(\frac{\pi d_{12}}{2H}\right). \tag{16}$$

Since one of the DRs is held at the CV center, in this new configuration the distance between them is $d_{12}/2$. The eigenvalue problem represented by Eq. (1) and the simplified Eq. (8) of the frequency of the TE^{+++} mode are solved for different separations of the $d_{12}/2$ variable. The results are plotted in Fig. 6, and compared to the values obtained using HFSS eigenmodes solver.

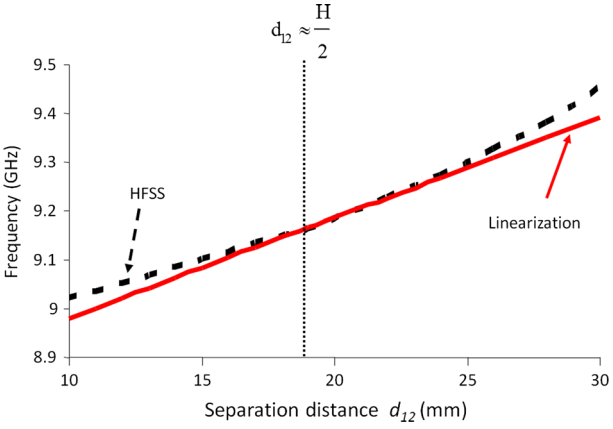

Fig. 5 Linearization of the frequency versus the separation distance for the TE^{+++} mode

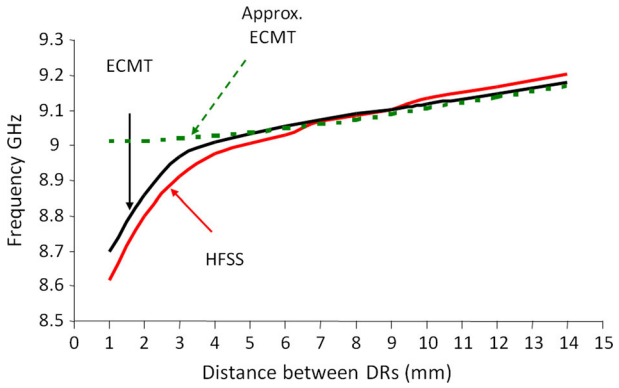

Fig. 6 Frequency change of the TE^{+++} mode as DR1 position changes along the cavity axis

Figure 6 indicates that the frequency of the TE^{+++} mode can be tuned over a substantial range (600 MHz) when DR1 is shifted relative to DR2 housed at the cavity center. This is better explained by referring to Eq. (8) of the mode frequency and the expression of β given by Eq. (16). As d_{12} increases, β decreases and from (Eq. 8) the frequency increases. However, when d_{12} is small (for this configuration <4 mm), κ_{12} cannot be ignored and the solution of Eq. (1) gives more reliable results, as Fig. 6 illustrates.

The eigenvector of the TE^{+++} mode, given by (Eq. 9), can be applied to find the electric field of the coupled mode. However, for EPR spectroscopy, one is more interested in the magnetic field component, which can be approximated as:

$$\bar{H}^{+++} = \frac{\beta}{\sqrt{\beta^2+1}}\bar{H}_1 + \frac{1}{\sqrt{\beta^2+1}}\bar{H}_2 + \bar{H}_3. \tag{17}$$

For a given $d_{12}/2$, β can be calculated from Eq. (16) and the magnitude of the magnetic field intensity is determined via Eq. (17). In Fig. 7, the calculation was carried out for $d_{12}/2 = 9$ mm and compared to those obtained using finite element simulation.

Figure 7 shows that the eigenvector calculated using Eq. (9) can be used to predict the profile of the fields of the TE^{+++} mode. For this particular configuration, DR1 acts as a frequency tuner. From (Eq. 16), $|\beta| \leq 1$, which according to (Eq. 17) implies that the magnetic field in the DR2 is always greater than the field in DR1 (tuner). The larger d_{12} is, the smaller β and consequently the energy stored in the tuner decreases until the TE^{+++} mode approaches the symmetric mode of the cavity-dielectric probe described in [8].

Finally one compares the filling factor of the two stacked dielectric resonators to a single dielectric resonator in a cylindrical cavity. The filling factor is defined as the integral of the stored energy in the magnetic field integrated over the sample volume divided by the energy stored in the whole cavity:

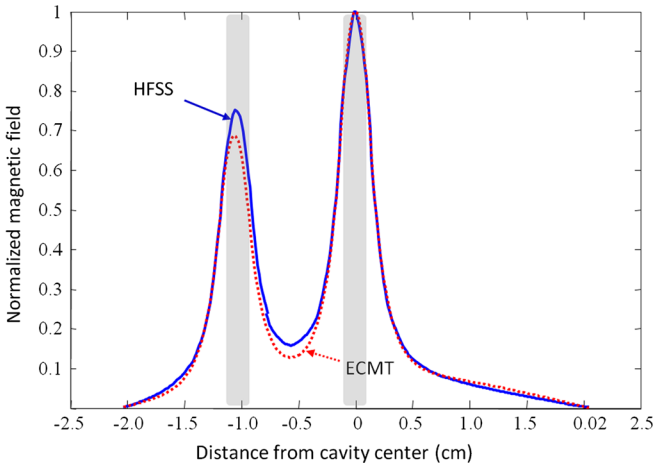

Fig. 7 Normalized magnitude of the magnetic field along the cavity axis using both ECMT and HFSS eigenmode solver. DR2 is fixed at the CV center and DR1 placed 9 mm away. The *shaded rectangles* highlight the positions of DR1 and DR2

$$\eta = \frac{\int_{V_{\text{Sample}}} |B_{1x}|^2 \mathrm{d}v}{\int_{V_{\text{Cavity}}} |B_{1x}|^2 \mathrm{d}v} = \frac{\int_{V_{\text{Sample}}} |H_{1x}|^2 \mathrm{d}v}{\int_{V_{\text{Cavity}}} |H_{1x}|^2 \mathrm{d}v},$$

here $B_{1x} = \mu_0 H_{1x}$. The time-averaged magnetic energy, W_{M}, stored in the entire DR/TE_{102} probe with volume, V_{Cavity}, is:

$$W_{\text{M}} = \frac{1}{4}\mu_0 \int_{V_{\text{Cavity}}} |H_{1x}|^2 \mathrm{d}v.$$

By comparing this equation to the denominator of the previous one and assuming that W_{M} is normalized to unity one gets [12]:

$$\eta \approx \frac{\pi r^2 \mu_0}{2} \int_0^{\ell} |H_{1x}|^2 \mathrm{d}x.$$

Here ℓ is the length of the sample and r is the radius of the DR2 inner hole. The term H_{1x} is the magnetic component of the exciting microwave field in the x-direction of the laboratory frame. In this case, it is equivalent to H_x^{+++}. By substituting Eq. (17) into this last equation one obtains:

$$\eta \approx \frac{\pi r^2 \mu_0}{2} \int_0^{\ell} \left| \left(\frac{\beta}{\sqrt{\beta^2+1}} H_1 + \frac{1}{\sqrt{\beta^2+1}} H_2 + H_3 \right) \right|^2 \mathrm{d}x.$$

In the case of a single resonator $\beta = 0$ and this equation reduces to:

$$\eta \approx \frac{\pi r^2 \mu_0}{2} \int_0^{\ell} |(H_2 + H_3)|^2 \mathrm{d}x.$$

From these last two equations and Fig. 7, it is clear that the probe's filling factor of the two stacked DRs in a CV is always lower than that of a single DR in a CV probe.

However, as the tuner resonator (DR1) is moved farther away from the CV center β decreases. Consequently its contribution diminishes and the filling factor increases. When DR1 gets very close to the CV wall, its contribution further decreases, due to the "image effect". The induced image across the cavity wall couples anti-symmetrically with the DR1 mode. This results in a significant reduction of the axial component of the DR1 magnetic field [7].

4 Summary and Conclusions

An EPR probe consisting of two stacked DRs placed in a CV is studied using ECMT. The coupled frequencies and eigenvectors are analytically derived.

For a specific separation distance between the two dielectrics, d_{12}, the two higher modes, TE^{++-} and TE^{+--}, are degenerate. Based on ECMT, the degeneracy condition occurs when $\kappa_{12} = \kappa_{13}$. In other words, when the coupling coefficient between the two dielectrics is equal to that of the dielectric-cavity pair.

From the eigenvector of the TE^{+--} mode, it is clear that this mode is completely dielectric in character and the cavity does not play any role in the coupling. This is attributed to the fact that the coupled energy pumped into the mode through the cavity is exactly equal to that pumped out of the mode back to the cavity. This is similar to the EIT-like system studied in [21, 22].

The frequency of the TE^{+++} mode is linear over a considerable separation distance d_{12}. Using ECMT, this linear relation was obtained and compared to finite element simulations. The mode shows a frequency change of 500 MHz when d_{12} changes by 2 cm. Thus, besides improving the signal-to-noise ratio this mode is ideal for EPR experiments when, a tuning capability of the probe is required [12].

Finally, the asymmetric configuration was studied. In this configuration, one of the resonators (DR2) was kept at the cavity center and the other was allowed to move along the cavity's z-axis. The resulting frequency curve indicates that indeed DR1 acts as a frequency tuner. The system's frequency changes approximately 600 MHz as the distance between the two DRs changes by 1.5 cm. Since the spatial magnetic field distribution is one of the most important parameters in EPR spectroscopy, a formula for the magnetic field along the cavity axis was proposed based on ECMT. The formula produces results that are in close agreement with those produced by a full-wave finite element simulator (HFSS). Thus, the electromagnetic field expressions and coupled frequencies can be applied to study complex EPR probes.

Acknowledgements SMM acknowledges the Natural Sciences and Engineering Research Council of Canada for financial support in the form of a discovery (operating) Grant. SMM also thanks the University of New Brunswick for the awards of Professor Emeritus and Honorary Research Professor. We would also like to acknowledge CMC Microsystems for providing the HFSS suite of programs that facilitated this research.

References

1. J.S. Hyde, W. Froncisz, T. Oles, J. Magn. Reson. **82**(1989), 223–230 (1969)
2. Y.E. Nesmelov, J.T. Surek, D.D. Thomas, J. Magn. Reson. **153**, 7–14 (2001)
3. A. Blank, E. Stavitski, H. Levanon, F. Gubaydullin, Rev. Sci. Instrum. **74**, 2853–2859 (2003)
4. I. Golovina, I. Geifman, A. Belous, J. Magn. Reson. **195**, 52–59 (2008)
5. R.R. Mett, J.W. Sidabras, I.S. Golovina, J.S. Hyde, Rev. Sci. Instrum. **79**, 94702 (2008)
6. S.Y. Elnaggar, R. Tervo, S.M. Mattar, IEEE Trans. Microw. Theory Tech. **63**, 2115–2123 (2015)
7. S.Y. Elnaggar, R. Tervo, S.M. Mattar, IEEE Trans. Microw. Theory Tech. **63**, 2124 (2015)
8. S.Y. Elnaggar, R. Tervo, S.M. Mattar, J. Magn. Reson. **238**, 1–7 (2014)
9. S.Y. Elnaggar, R. Tervo, S.M. Mattar, J. Magn. Reson. **242**, 57–66 (2014)
10. S.Y. Elnaggar, R. Tervo, S.M. Mattar, J. Magn. Reson. **245**, 50–57 (2014)
11. J.S. Colton, L.R. Wienkes, Rev. Sci. Instrum. **80**, 035106 (2009)
12. S.M. Mattar, S.Y. Elnaggar, J. Magn. Reson. (San Diego Calif.: 1997) **209**(2011), 174–182 (2011)
13. S.M. Mattar, A.H. Emwas, Chem. Phys. Lett. **368**, 724–731 (2003)
14. A. Sienkiewicz, M. Jaworski, B.G. Smith, P.G. Fajer, C.P. Scholes, J. Magn. Reson. **143**, 144–152 (2000)
15. A. Sienkiewicz, K. Qu, Rev. Sci. Instrum. **65**, 68–74 (1994)
16. A. Sienkiewicz, B. Vileno, S. Garaj, M. Jaworski, L. Forró, J. Magn. Reson. **177**, 261–273 (2005)
17. S.B. Cohn, Microw. Theory Tech. **16**, 218–227 (1968)
18. M. Jaworski, A. Sienkiewicz, C.P. Scholes, J. Magn. Reson. (1969–1992) **124**, 87–96 (1997)
19. A.J.S. Fiedziuszko, IEEE Trans. Microw. Theory Tech. **19**, 779–781 (1971)
20. S.Y. Elnaggar, R.J. Tervo, S.M. Mattar, J. Appl. Phys. **118**, 194901 (2015)
21. R.E. Hamam, A. Karalis, J.D. Joannopoulos, M. Soljačić, Ann. Phys. **324**, 1783–1795 (2009)
22. S.Y. Elnaggar, J. Appl. Phys. **121**, 064903 (2017)
23. I. Awai, IECIE Trans. Electron **E88-C**, 2295–2301 (2005)